Journal of Thermal Analysis and Calorimetry, Vol. 79 (2005) 605–613

NANO-WATT STABILIZED DSC AND ITS APPLICATIONS

S. Wang, K. Tozaki, H. Hayashi and H. Inaba[*]

Faculty of Education, Chiba University, 1-33 Yayoi-Chou, Inage-ku, Chiba 263-8522, Japan

A high sensitivity and high resolution DSC working between 220 and 400 K with a baseline stability of ±3 nW for many hours, with a low noise of nV order, with a quick response time of 2 s and with the temperature resolution of 0.1 mK, capable of measuring in the both direction of heating and cooling has been designed and constructed. The stability of the baseline was achieved by the use of a high sensitive temperature sensor, a precise temperature control of ±0.1 mK, a semi-adiabatic control, the damping devices to decrease the temperature fluctuation at the sample cell and the devices to decrease noises on the lead wires. The specific heat capacity of a single crystalline alumina was measured with an inaccuracy of 1% by the use of the DSC. Very fine structures of phase transitions were observed at a cooling rate of 5 μK s^{-1} in the measurement of $C_{22}H_{46}$ by application of the high sensitivity DSC. The measurement for very small samples of μg order has become possible using the high sensitivity DSC and the application for the melting transition of $C_{15}H_{31}COOH$ and $C_{32}H_{66}$ was presented.

Keywords: *high resolution-DSC, high sensitivity-DSC, phase transition, small sample*

Introduction

The heat flux differential scanning calorimetry (DSC) is a technique to measure the temperature difference between a sample and a reference material due to heat generated from or absorbed in the sample under the controlled temperature program [1, 2]. The temperature difference between the sample and the reference material is converted to heat flux by the use of a proper calibration. It has given important information in the fields of polymer science, biological science, pharmaceutical science, metal science, inorganic science and their related industries by measuring heat absorbed or generated due to melting, glass transition, phase transitions and chemical reactions [1–8]. The demands for a highly sensitive DSC are increasingly great in various fields in order to detect very small heat effects. The merits of the high sensitivity DSC would be the measurement of a very small heat such as an enzyme reaction, the phase transition of monolayer [9], interface reactions, phase transitions with very small enthalpy change [9, 10] and small samples of less than 0.1 mg. The sensitivity of the DSC, however, is determined by the baseline stability and it is several μW in the commercial DSC made by major manufacturers according to Wunderich [1] and 0.4 μW in the high-sensitive DSC made by Privalov according to Hatakeyama and Quinn [2]. The sensitivity of the DSC by Privalov was improved by increasing the sample size and using several thermocouples connected in series to measure the temperature difference between a sample and a reference material. However, to increase the sample size is not desirable in the view of the resolution of the calorimeter for the sample with multiple phase transitions, since the temperature distribution becomes large in the large sample. Moreover, the calorimeter is desirable to have enough sensitivity for a very precious small sample less than 0.1 mg. In the commercial DSC, the heating rate is usually chosen to be larger than 0.1 K min^{-1} [1–8] in order to obtain a significant signal, since the magnitude of the signal is proportional to the heating rate. In the high heating rate, however, the temperature distribution in the sample becomes large, and the peak temperature rises so that the resolution of the calorimeter becomes bad. When the heating rate is chosen to be very slow, the drift of the baseline would become relatively large. If the response time of the calorimeter is long, the resolution of the calorimeter becomes bad.

It is desirable, therefore, to develop a high sensitivity and high resolution DSC capable of measuring a small heat with a small baseline fluctuation, a small drift of the baseline and a quick response time at a slow heating rate using small amount of sample. It is also desirable to develop a high sensitivity and high resolution DSC capable of measuring in the both direction of heating and cooling, since some sorts of materials in the cooling process often show a different behavior from that in the heating process [9–12].

In this study, we would like to describe the design and construction of a high sensitivity and high resolution DSC capable of measuring a small heat

* Author for correspondence: inabah@faculty.chiba-u.jp

1388–6150/$20.00

Akadémiai Kiadó, Budapest, Hungary
Springer, Dordrecht, The Netherlands

with a baseline stability of several nW and a quick response time of 2 s and with a temperature resolution of less than 0.1 mK at a very slow scan rate such as 5 μK s^{-1} (0.3 mK min^{-1}) in the both direction of heating and cooling. We also would like to show some applications of the high sensitivity and high resolution DSC for samples with very fine structures of phase transitions and for very small samples of μg order.

Design principle of a high sensitivity DSC

The heat flux DSC measures the temperature difference between a sample and a reference material due to heat generated from or absorbed in the sample as a function of time. The differential heat flux between the sample and the reference one, dQ/dt, is proportional to the temperature difference between the sample and the reference material, ΔT, assuming a steady state, the mass of the sample container to be equal to that of the reference material and the heat capacity of the reference material to be zero:

$$\mathrm{d}Q/\mathrm{d}t = -\Delta T/R = Cs\,\mathrm{d}T/\mathrm{d}t \quad (1)$$

where the negative sign means that the temperature of the sample side becomes lower at a heating run, R is the thermal resistance between the sample cell and the thermal block and Cs is the net heat capacity of the sample. The temperature difference, ΔT is represented by the potential difference ΔE of the temperature sensor between the sample and the reference material as:

$$\Delta T = \Delta E/S \quad (2)$$

where S is the thermoelectric power of the temperature sensor. Combining Eqs (1) and (2), we obtain

$$\mathrm{d}Q/\mathrm{d}t = -\Delta E/(RS) \quad (3)$$

Equation (3) is rewritten by putting the product of R and S to be K as:

$$\Delta E = -(RS)\mathrm{d}Q/\mathrm{d}t = -K\mathrm{d}Q/\mathrm{d}t \quad (4)$$

Equation (4) shows that the sensitivity of the calorimeter is proportional to the apparatus constant K, which is the product of R and S and is determined by the measurement of calibration. In order to increase the sensitivity of the calorimeter, K, the thermal resistance between the sample cell and the thermal block and the thermoelectric power of the temperature sensor should be large. Since the thermal resistance between the sample cell and the thermal block is mainly determined by the thermal conductivity of the temperature sensor, the choice of the temperature sensor is very important in the design of the calorimeter. In the commercially available DSC [1, 2], the temperature sensors such as a chromel–alumel thermocouple and a thermopile with multi-junction thermocouples have been used. When a thermopile with multi-junction thermocouples is used, the thermoelectric power S would be increased but the size of the sample cell would be increased and the thermal resistance R may be decreased. In order to increase S without decreasing R, the use of the temperature sensor with the thermoelectric power larger than thermocouple is desirable. The use of a semiconducting thermoelectric module as a temperature sensor is one of the choices, although the temperature range usable is limited. The output voltage of a semiconducting thermoelectric element is about 0.44 mV K^{-1}, for example, being 11 times larger than that of a usual thermocouple, 40 μV K^{-1}.

Another point to increase the sensitivity of the calorimeter is to decrease various noises and the drift of the baseline. The main sources of the noises and the drift of the baseline in the DSC would be as follows.

- The noise due to the fluctuation of the temperature control
- The electric noise and thermoelectric noise on the lead wires and on the measuring system and
- The drift of the baseline due to the heat leak from or to the surroundings

The noise due to the fluctuation of the temperature control may be primarily determined by the control error in the heating or cooling element. The best temperature control in the heating or cooling would be about ±0.1 mK in real systems. The maximum noisy temperature difference permitted between the sample and the reference material to construct a nW-stabilized DSC, however, would be ±1 μK, as will be described later in detail. This means that the temperature fluctuation at the sample cell must be reduced by at least two orders of magnitude and some damping devices between the heating/cooling element and the sample cell are necessary. We have chosen the pairs of a thermoelectric module and a thick Cu block for that purpose. They work as the damping devices by integrating the temperature fluctuation with a time constant CR_t, where C is a heat capacity and R_t is a thermal resistance determined by the pairs of the thermoelectric module and the thick Cu block. The combination of C and R_t can be regarded to be the same as the integral circuit with the capacitance C and resistance R_t in an equivalent circuit.

The electric noise and thermoelectric noise on the lead wires and on the measuring system should also be minimized to construct the high sensitivity DSC. The choice for the path and the diameter of the lead wires for the differential signal between the sample cell and the reference cell is extremely important. The junction between different metals such as soldering should be avoided especially for the place under a large temperature fluctuation because of the thermoelectric noise. If

such a junction cannot be avoided, the junction points of the two lead wires must be kept at the same thermal condition as possible by some means. In order to decrease the drift of the baseline due to the heat leak from or to the surroundings, another temperature control and thermal shields between the sample cell and the enclosing shield case are necessary.

Construction of the high sensitivity DSC

A high sensitivity and high resolution DSC has been constructed as shown in Fig. 1, considering the design principle described above. The calorimeter was set in a refrigerating vessel, V2 in order to extend the temperature range to temperatures as low as 220 K. The heating or cooling rate was mainly controlled by controlling the current of thermoelectric module, TM5, using Pt resistance thermometer, TS3. Since TM5 can pump heat in either direction to heat or cool the copper blocks by changing the direction of the current through it, the measurement in the both direction of heating and cooling is possible with this apparatus. Since the power of TM5 is not enough to attain to 400 K and the precision of the temperature control is not enough by the single control using TM5 only, an auxiliary temperature control was made by controlling the current of a heater H1 using a Pt resistance thermometer, TS2. The temperature of the thick metal

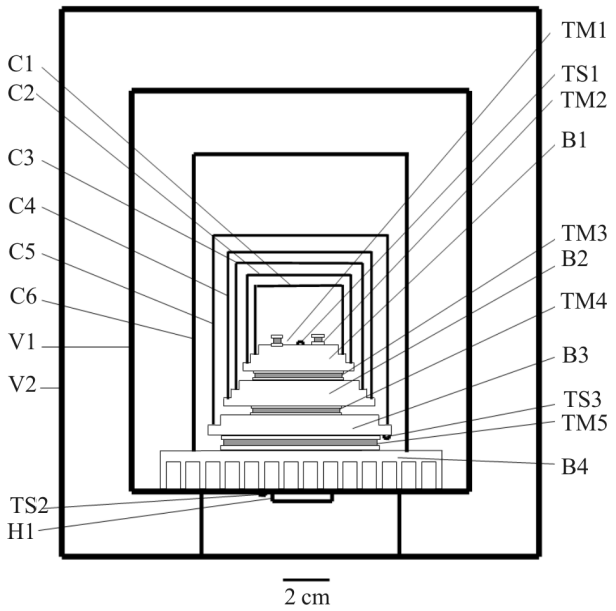

Fig. 1 Schematic drawing of the high sensitivity and high resolution DSC. TS1~3; Pt resistance thermometers, C1~6; copper shields, B1~3; copper blocks, B4; an aluminum block, TM1 and TM2; semiconducting temperature sensors, TM3~5; semiconducting thermoelectric modules, H1; heater, V1; enclosing metal shield case, V2; refrigerating vessel

shield case, V1 was controlled to be almost the same as the temperature of TS3, keeping a nearly adiabatic condition in the central parts of the calorimeter.

The temperature difference between a test sample and a reference material, produced by the heat absorbed in or released from the sample, was measured by thermoelectric modules, TM1 and TM2 (Ferrotec Co. 9500/018/012), which are made of 18 semiconducting thermoelectric elements made of BiTe connected in series. The output voltage of the thermoelectric module is about 8 mV K^{-1}. The temperature of the sample was measured using a Pt resistance thermometer, TS1, which was regarded as the temperature of the sample.

The pairs of the thermoelectric module and the thick Cu block, TM4 and B2 and TM3 and B1 were used for the damping devices to decrease the temperature fluctuation of the sample cell resulting from the temperature fluctuation at TS3, where the rate control of heating or cooling was made. The thick Cu blocks work mainly as a large heat capacity and the thermoelectric module as a thermal resistance.

In order to reduce the electric noise and thermoelectric noise on the lead wires in the measuring system, the path and the diameter as well as the junction points of the lead wires for the differential signal between the sample and the reference cells were carefully chosen. A digital voltmeter of Keithley 2001 with a low noise amplifier (1801), which has the sensitivity of 0.1 nV and the precision of 0.03%, was chosen for the measurement of the differential temperature between the sample and reference cells. The auxiliary temperature control using the heater H1 served to decrease the drift of the baseline due to the heat leak from or to the surroundings keeping a semi-adiabatic condition. Thermal shields, C1, C2, C3, C4, C5 and C6 made of Cu were placed between the base block and the enclosing shield case, V1 to decrease the drift of the baseline due to the heat leak. The refrigerating vessel, V2 worked to decrease the drift of the baseline by reducing the temperature change in the calorimeter due to the change of room temperature.

Performance of the high sensitivity DSC

The performance of the high sensitivity DSC was checked by measuring the temperature changes of various points and the stability of the baseline. The temperature changes at the enclosing shield case, V1 and the base copper block, B3, were measured by Pt resistance thermometers, TS2 and TS3, respectively, as shown in Fig. 2, where the temperature fluctuation of TS2 and TS3 are seen to be within ±1 and ±0.1 mK, respectively. The calibration of the heat flux of this DSC was made at the heating rate of 1 mK s^{-1} (0.06 K min^{-1}) by using a single alumina crystal. The alumina sample was enclosed in the open-type com-

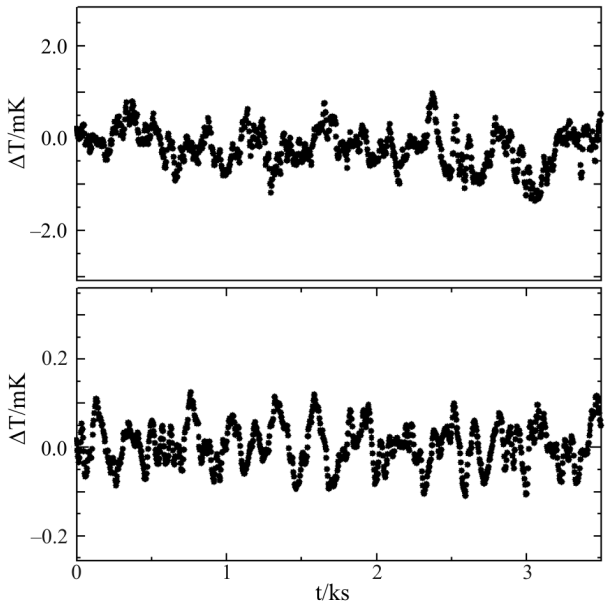

Fig. 2 Temperature variations of rough and precise control. The upper and lower figure shows the temperature variation at TS2 and TS3, respectively

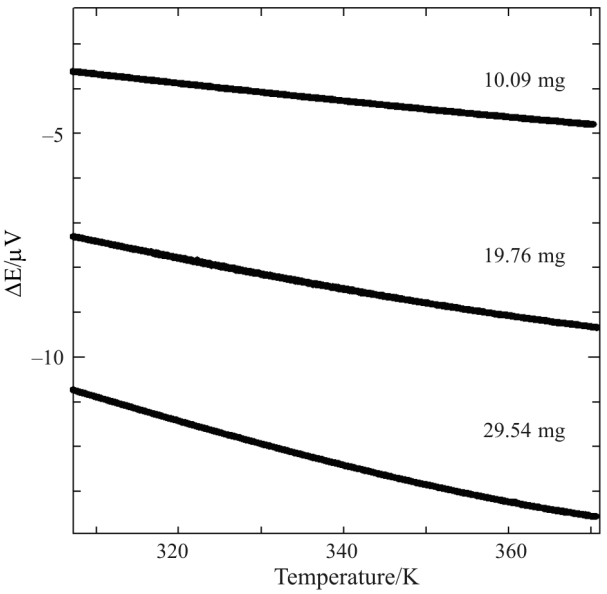

Fig. 3 Difference of electromotive force between the temperature sensors, TM1 and TM2, in the measurements for different masses of single crystalline alumina, 10.09, 19.76 and 29.54 mg

mercially available aluminum container with the diameter of 4.5 mm and the depth of 1.8 mm and almost the same mass of the empty aluminum container within the difference of 0.01 mg was chosen for the reference material. The results of the measurement of calibration for different masses of the alumina samples: 10.09, 19.76 and 29.54 mg are shown in Fig. 3. The difference of the differential voltage between TM1 and TM2, $\delta(\Delta E)$, due to the difference of the heat capacity of alumina for the different masses becomes the following combining Eqs (1) and (4),

$$\delta(\Delta E) = -K\delta(\mathrm{d}Q/\mathrm{d}t) = K\delta(Cs\,\mathrm{d}T/\mathrm{d}t) \qquad (5)$$

where the notation δ means the difference due to the different mass of alumina.

We used the difference of ΔE between the measurements of the alumina samples: 10.09 and 19.76 mg to determine the apparatus constant K. Substituting the difference of ΔE between the measurements of the alumina samples: 10.09 and 19.76 mg as shown in Fig. 3, the calculated differential heat capacity of alumina due to the difference of the mass using the reference values [13], and the heating rate of 1 mK s^{-1} for Eq. (5), the apparatus constant K was determined. The result is shown in Fig. 4, where that of the commercial heat flux DSC of Rigaku 8230 is also shown for comparison. The apparatus constant K of the present DSC is an increasing function with temperature, while K of the commercial DSC is a decreasing function with temperature. This is due to the fact that the temperature sensor for the present DSC is made of a semiconducting material and that for the commercial DSC is a thermocouple. The apparatus constant K of the high sensitivity DSC is about 550 times

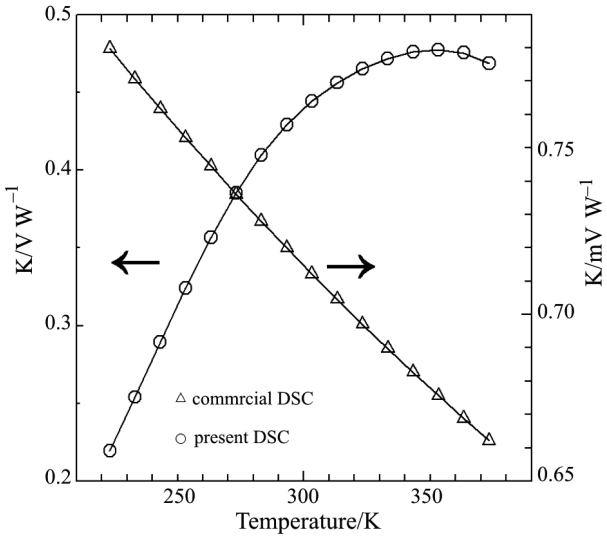

Fig. 4 Apparatus constant K of the present DSC comparing with that of a commercial DSC. The right ordinate is for a commercial DSC, whose unit is three orders of magnitude smaller than of the left one

larger than that of the commercial DSC at 300 K. Substituting the calibrated factor K thus determined, the difference of ΔE between the measurements of the alumina samples: 19.76 and 29.54 mg, and the heating rate of 1 mK s^{-1} for Eq. (5), the specific heat capacity of alumina was obtained as shown in Fig. 5, where the reference data [13] are also shown. The present data are seen to be within an inaccuracy of 1%.

The stability of the baseline in the present DSC was measured at about 300 K as shown in Fig. 6,

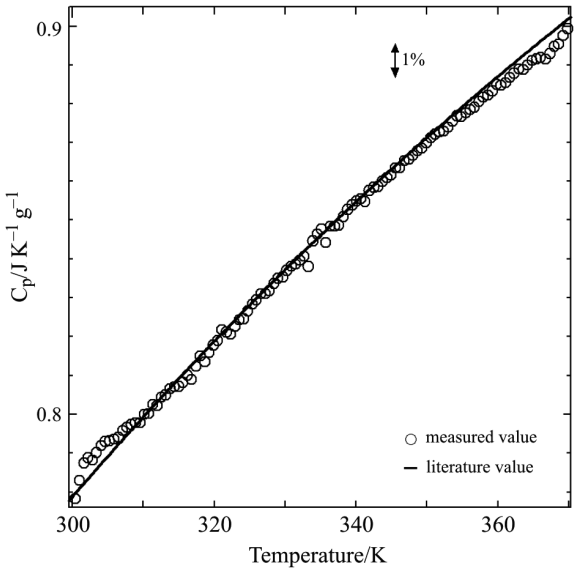

Fig. 5 Specific heat capacity of a single crystalline alumina together with the reference data [13]

where that in the commercial DSC is also shown for comparison. The stability of the baseline in the present DSC is seen to be within ±3 nW. Although the stability of the baseline is only shown for 3 h in Fig. 6, for 48 h it was almost the same as that shown in Fig. 6. The stability of the baseline in the commercial DSC is within ±2 μW, which is the same order of magnitude in the commercial apparatus made by major manufacturers according to Wunderich [1]. The ratio of the stability of the present DSC to the commercial one is 670, and it is the same order as the ratio of the apparatus constant *K*, 550, as seen in Figs 4 and 6.

The response time of the calorimeter is also an important factor of a calorimeter, since it is one of the major factors to determine the resolution of the calorimeter. The response time of the present DSC was estimated to be about 2 s as will be shown later. The resolution of the calorimeter is determined as the composite properties of the response time, the sample amount, the sensitivity and the noise level of the calorimeter and it was estimated to be less than 0.1 mK as will be shown later, indicating the excellent performance of the present DSC.

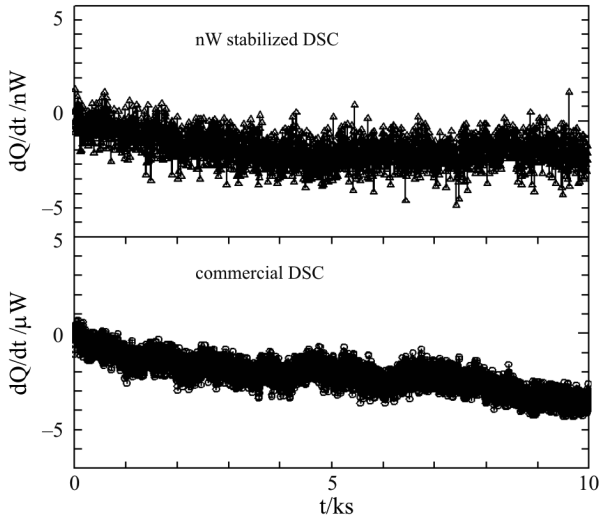

Fig. 6 Baseline stability of the present DSC and the commercial DSC

Some applications of the high sensitivity DSC

Measurement of docosane

The docosane ($C_{22}H_{46}$) sample with the purity of 99.999% purchased from National Institute of Standards and Technology. The sample container used was a commercially available aluminum container with the diameter of 4.5 mm and the depth of 1.8 mm. The lid has a flat shape and was sealed to the upper flat end of the container by pressing. The sample amount was 1.28 mg and the DSC measurement was made at the cooling rate of 0.5 mK s^{-1} (0.03 K min^{-1}) and 5 μK s^{-1} (0.3 mK min^{-1}). The results for the cooling rate of 0.5 mK s^{-1} are shown in Fig. 7, where five peaks due to phase transitions are seen. The peak 2 is due to the liquid to solid transition and the peaks 3–5 are concerned with rotator transitions, where the alkane chains undergo the unrestricted random rotation holding the trans-zigzag conformation [14, 15]. The peak 1 is seen about 3 K higher than the melting point due to the formation of monolayer solid on the liquid surface, which has been confirmed by the measurements of X-ray diffraction, surface tension and molecular dynamics simulation [16–20]. Detection of the small peak due to such a two-dimensional phase

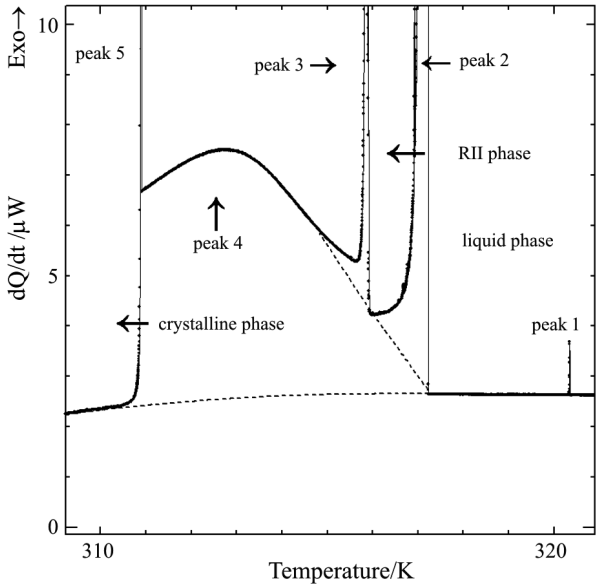

Fig. 7 DSC curve of $C_{22}H_{46}$ at the cooling rate of 0.5 mK s^{-1}, showing five peaks due to phase transitions

transition shows a high sensitivity of the present DSC. The results for a cooling rate of 5 μK s^{-1} around 315.9 K are shown in Fig. 8, where the peak 3 is seen to be composed of many sharp peaks. This would suggest that CH_2 elements in the different positions in the $C_{22}H_{46}$ molecule have slightly different transition temperatures in the transition from the rotator phase II (RII) to the rotator phase I (RI), which can only be detected by a very slow cooling rate. The detection of the many sharp peaks shows a quick response and an enough resolution of the present DSC. One of the sharp peaks around 315.933 K with a magnified horizontal axis is shown in Fig. 9, where the response of the rising peak at about 315.9329 K is estimated to be within 10 μK corresponding to the response time of 2 s and the resolution of the temperature is estimated to be less than 0.1 mK. It is noted here that the fluctuation of the baseline in Fig. 8 is within several nW, showing the same order of stability as the measurement at a constant temperature shown in Fig. 6. The baseline stability within several nW lasted more than 24 h, although it cannot be seen in Fig. 8.

Measurements for very small amount of samples

When the sensitivity of DSC is high enough, it would become possible to measure a very precious sample with an amount of μg order. The measurements on $C_{15}H_{31}COOH$ and $C_{32}H_{66}$ samples with an amount of μg order were made for that purpose. The $C_{15}H_{31}COOH$ sample with the purity of 99.5% was purchased from Tokyo Kasei Kogyo Co. Inc., and $C_{32}H_{66}$ sample with the purity of 99.6% was synthesized by using Wurtz

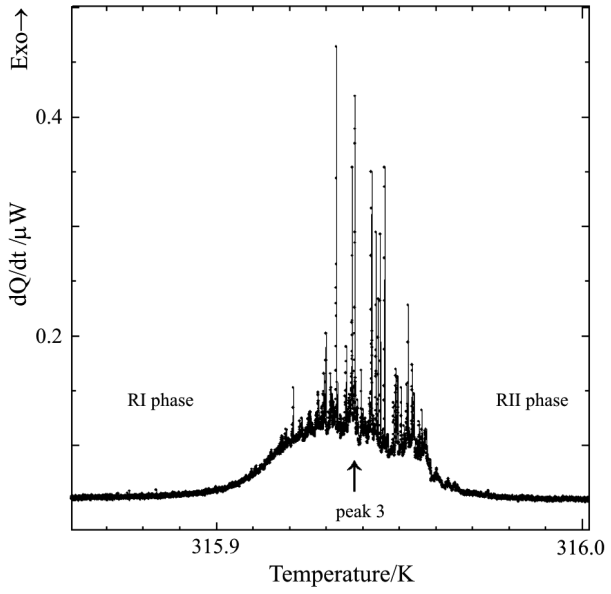

Fig. 8 DSC curve of $C_{22}H_{46}$ around 315.95 K at the cooling rate of 5 μK s^{-1}

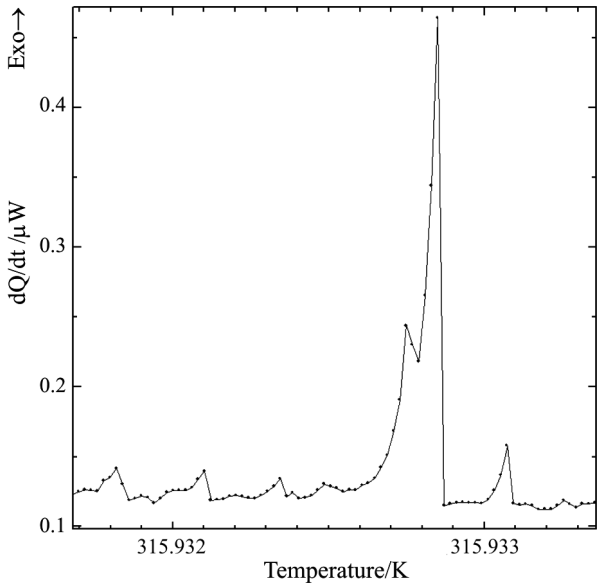

Fig. 9 The magnified DSC curve around 315.933 K of Fig. 8

condensation method [10]. The weighed sample was dissolved into a volume of hexane, a known volume of the solution was transferred into an aluminum container using a microcylinder, and then the mass of the sample in the Al container was calculated. The sample container used was a commercially available aluminum container with the diameter of 4.5 mm and the depth of 1.8 mm. The lid has a flat shape and was sealed to the upper flat end of the container by pressing after the solvent was fully evaporated. The results of the DSC measurements for the $C_{15}H_{31}COOH$ sample with the amount from 0.57 to 7.60 μg at the heating rate of 0.5 mK s^{-1} are shown in Fig. 10, where the endothermic peak shifts to a low temperature and becomes smaller as the sample amount decreases. The largest endothermic peak due to melting is seen at 335.96 K for the sample of 7.60 μg, which is slightly lower than the value of a bulk sample, 336.15 [21] and 337 K [8]. The melting enthalpy is calculated as 45.6 kJ mol^{-1}, which is considerably smaller than that of the bulk sample, 53.4 kJ mol^{-1} [8].

The results of the DSC measurements at the heating rate of 0.5 mK s^{-1} from 339.1 to 343.8 K for $C_{32}H_{66}$ sample with the amount from 1.85 to 14.72 μg are shown in Fig. 11, where the endothermic peak around 339.4 K shows the crystal-rotator transition and that around 343.7 K shows the melting transition [10]. Figure 11 shows that the two transitions change similarly and irregularly with the sample amount, being different from the case of $C_{15}H_{31}COOH$. The melting enthalpy for the sample amount of 14.72 μg is calculated as 74.8 kJ mol^{-1}, slightly smaller than that of the bulk sample, 79.7 kJ mol^{-1} [10]. The melting temperatures of both $C_{15}H_{31}COOH$ and $C_{32}H_{66}$ samples are plotted *vs*. logarithm of the sample amount as shown in Fig. 12, where the results for the sample amounts of mg

order are also shown. It is apparently seen in Fig. 12 that the melting temperature of $C_{15}H_{31}COOH$ decreases monotonously with the decrease of the sample amount. In the case of $C_{32}H_{66}$, however, the melting temperature changes irregularly when logarithm of the sample amount is less than 1.2, and it increases as the sample amount increases. The melting enthalpies of both $C_{15}H_{31}COOH$ and $C_{32}H_{66}$ samples are plotted *vs*. logarithm of the sample amount as shown in Fig. 13. It is found that the melting enthalpy of $C_{15}H_{31}COOH$ decreases with the decrease of the sample amount and becomes only 16.4 kJ mol^{-1} at the sample amount of 0.57 μg, being about one third of the bulk. The melting enthalpy of $C_{32}H_{66}$ also decreases with the decrease of sample amount, but the change is smaller than that of $C_{15}H_{31}COOH$.

When the sample amount becomes very small, the number of $C_{15}H_{31}COOH$ or $C_{32}H_{66}$ molecules near the bottom surface of the Al container relatively increases and the molecules in the solid state are disordered due to the interaction with the Al container, resulting in lowering the melting temperature and the decrease in

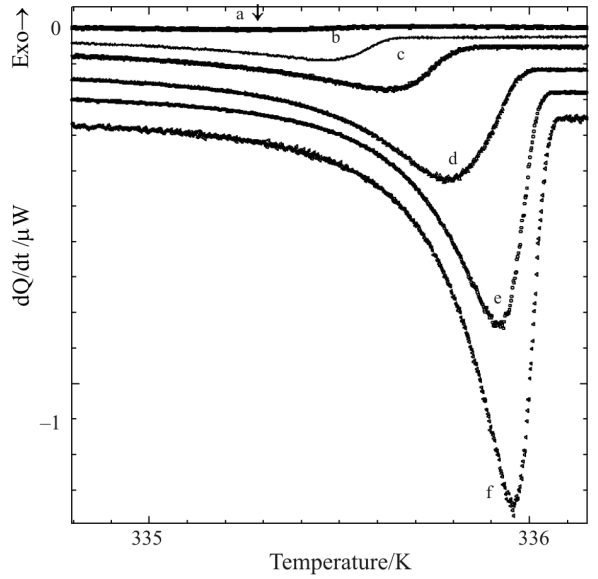

Fig. 10 DSC curves of $C_{15}H_{31}COOH$ at the heating rate of 0.5 mK s^{-1} for various amount of samples. a – 0.57 μg, b – 1.52 μg, c – 2.28 μg, d – 3.8 μg, e – 5.70 μg, f – 7.60 μg

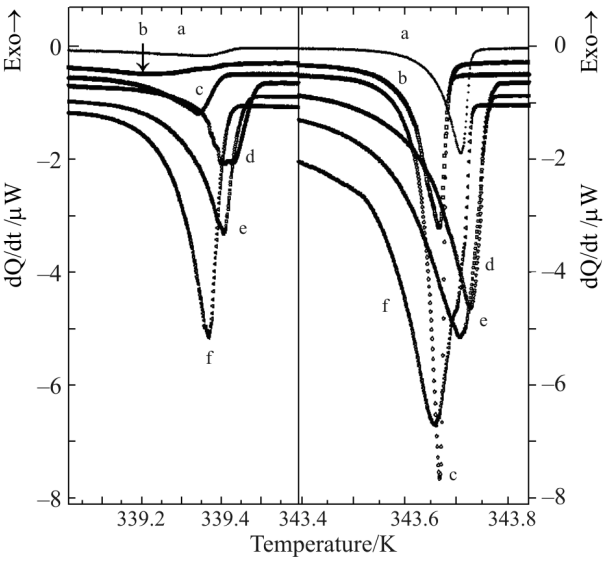

Fig. 11 DSC curves of $C_{32}H_{66}$ at the heating rate of 0.5 mK s^{-1} around the solid–solid transition (339.4 K) and the melting transition (343.7 K) for various amount of samples. The intermediate temperature range from 339.6 to 343.4 K is omitted in the figure. a – 1.85 μg, b – 2.95 μg, c – 4.43 μg, d – 7.38 μg, e – 11.07 μg, f – 14.72 μg

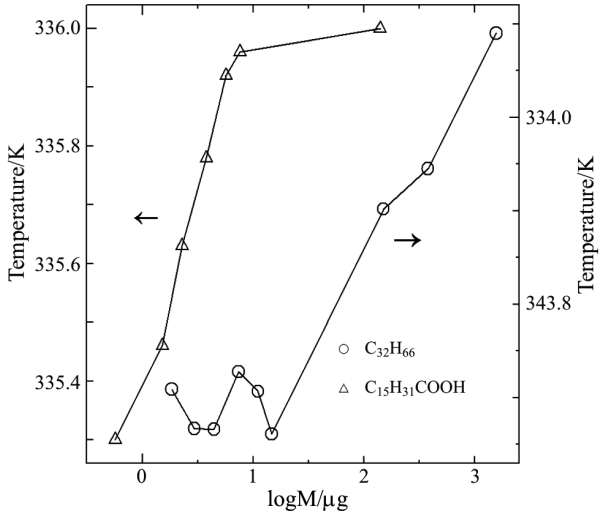

Fig. 12 Melting point of $C_{15}H_{31}COOH$ and $C_{32}H_{66}$ as a function of logarithm of the sample amount. The left ordinate is for $C_{15}H_{31}COOH$ and the right ordinate is for $C_{32}H_{66}$

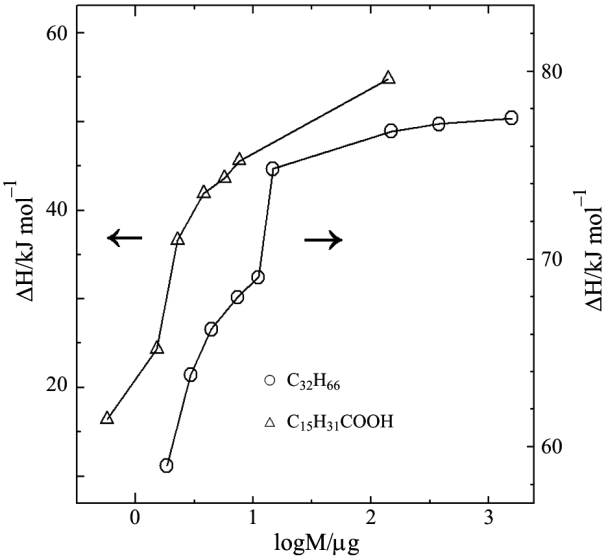

Fig. 13 Melting enthalpy of $C_{15}H_{31}COOH$ and $C_{32}H_{66}$ as a function of logarithm of the sample amount. The left ordinate is for $C_{15}H_{31}COOH$ and the right ordinate is for $C_{32}H_{66}$

the melting enthalpy. The fact that lowering the melting temperature as a function of the sample amount is monotonous and the decrease of the melting enthalpy is large in $C_{15}H_{31}COOH$ as compared with $C_{32}H_{66}$ may be related with the existence of a hydrophilic carboxy group in $C_{15}H_{31}COOH$. Since the bottom surface of the Al container is considered to have a hydrophilic hydroxy group, the $C_{15}H_{31}COOH$ molecules may be apt to be oriented along the bottom surface of the Al container by an attractive interaction between carboxy group in $C_{15}H_{31}COOH$ molecule and hydroxy group on the Al container. Since the bottom surface of the Al container is considered to have a roughness of μm order, the interaction may cause a large disorder in the $C_{15}H_{31}COOH$ molecules near the bottom surface of the Al container. On the other hand, $C_{32}H_{66}$ molecules do not have any hydrophilic part and then the interaction between $C_{32}H_{66}$ molecules and the Al container is considered to be weak. Therefore, the orientation of $C_{32}H_{66}$ molecules near the bottom surface of the Al container is considered to be dependent on the contact of the sample with the bottom surface of the Al container and on the shape of the sample, and then the melting point as a function of the sample amount changes irregularly as seen in Figs 11 and 12. The smaller decrease of the melting enthalpy at small amount of samples in $C_{32}H_{66}$ as compared with $C_{15}H_{31}COOH$ is considered to be due to the smaller interaction with the Al container.

Discussion

The estimation and the measurement of the noise level in the output signal and the temperature fluctuation at the sample cell is very important in order to achieve the baseline stability of nW-level. In the present DSC, the measurement was made with the baseline stability of ±3 nW as seen in Fig. 6. The noise level in the output signal and the temperature fluctuation at the sample cell can be estimated using this value as follows.

Since the apparatus constant K is 0.44 (V W^{-1}) at 300 K as seen in Fig. 4, the noise level of the output voltage of the temperature sensor between the sample cell and the reference one becomes 0.44 (V W^{-1}) ·(±3 nW)=±1.3 nV at 300 K according to Eq. (5). To make the measurement at the electric and thermoelectric noise level of 1.3 nV is very difficult, because such a low voltage of signal would easily be disturbed by these noises on the lead wires in the measuring system. When the measurement is made with the baseline stability of ±3 nW, the temperature fluctuation at the sample cell measured as the difference between the sample and the reference one is determined as (±1.3 nV)/(8 mV K^{-1})=±0.16 μK at 300 K using Eq. (2) and the value of ±1.3 nV for ΔE and 8 mV K^{-1} for S. To achieve the temperature fluctuation of ±0.16 μK at the sample cell is extremely difficult, since such a small temperature fluctuation cannot be realized by a usual temperature control. However, the use of the damping devices with the pairs of the thermoelectric module and the thick Cu block working as the integral circuit was effective to achieve the temperature fluctuation of ±0.16 μK at the sample cell in the present DSC.

We would like to discuss a critical factor to obtain the baseline stability of several nW here. The factors to determine the baseline stability of the present DSC would be the precision of temperature control, the effectiveness of damping devices to reduce the temperature fluctuation at the sample cell, the sensitivity of the temperature sensor at the sample and reference material cells and the devices to reduce the electric and thermoelectric noises on the lead wires in the measuring system.

The first two factors: the precision of temperature control and the effectiveness of damping devices would determine the real temperature stability at the sample and reference material cells. The precision of temperature control is in the range of ±0.1 mK, which cannot be reduced largely in real systems. On the other hand, the damping devices are the pairs of the thermoelectric module and the thick Cu block, which can be changed to obtain an optimum condition. Therefore, the real temperature stability at the sample and reference material cells can be kept within a limited error and the first two factors would not be critical ones to determine the baseline stability. In reality, the temperature fluctuation at TS3 seems not to affect the baseline fluctuation. The shape of the temperature fluctuation at TS3 seen in Fig. 2 is different from that of the baseline fluctuation seen in Fig. 6.

The last two factors: the sensitivity of the temperature sensor at the sample and reference material cells and the devices to reduce the electric and thermoelectric noises on the lead wires in the measuring system would determine the magnitude of the output voltage to that of the noises in a condition that the temperature difference between the sample and the reference material is constant. The signal to noise ratio increases either when the sensitivity of the temperature sensor increases or when the electric and thermoelectric noises decrease. When the room temperature was largely changed, the baseline drifted significantly probably due to the thermoelectric noise. Therefore, the devices to reduce the electric and thermoelectric noises on the lead wires in the measuring system are considered to be a critical factor to determine the baseline stability in the present DSC.

The fluctuation of the baseline was within several nW in the measurement of $C_{22}H_{46}$ as shown in Fig. 8.

This result shows that the DSC was constructed and worked as designed. It should be noted, however, that the baseline stability of nW-order becomes bad in the case of a rapid change of room temperature probably due to the drift in the measuring system.

Conclusions

A high sensitivity and high resolution DSC working between 220 and 400 K capable of measuring a small heat using small samples less than 0.1 mg at a very slow scan rate such as 5 μK s^{-1} (0.3 mK min^{-1}) in the both direction of heating and cooling has been designed and constructed. The DSC has a quick response time of 2 s and a temperature resolution of less than 0.1 mK. The stability of the baseline, ±3 nW, was achieved by the use of a high sensitive temperature sensor with the thermoelectric power of 8 mV K^{-1}, a precise control keeping the temperature to be ±0.1 mK by controlling the current of a thermoelectric module, another control keeping the central parts of the calorimeter to be nearly in adiabatic condition, the damping devices to decrease the temperature fluctuation at the sample cell and a low noise nano-voltmeter together with some devices to reduce the electric and thermoelectric noises on the lead wires in the measuring system. The sensitivity and the stability of the present DSC were more than 500 times larger than those of a commercial DSC. The specific heat capacity of a single crystalline alumina was measured with an inaccuracy of 1% using the DSC.

Very fine structures of phase transitions were observed at a heating or cooling rate of 5 μK s^{-1} in the measurement of $C_{22}H_{46}$ by application of the DSC. The melting transition of $C_{15}H_{31}COOH$ and $C_{32}H_{66}$ was observed using samples of μg order, although the melting peak decreases and shifts to the low temperature side as the sample amount decreases due to the interaction with the bottom of Al container.

References

1 B. Wunderich, 'Thermal Analysis', Academic Press, New York 1990.
2 T. Hatakeyama and F. X. Quinn, 'Thermal Analysis: Fundamentals and Application to Polymer Science', Wiley, New York 1994.
3 W. L. Jarrett, L. J. Mathias, R. G. Alamo, L. Mandelkern and D. L. Dorset, Macromolecules, 25 (1992) 3468.
4 P. Barbillon, L. Schuffenecker, J. Dellacherie, D. Balesdent and M. Dirand, J. Chem. Phys., 88 (1991) 91.
5 U. Domanska and D. Wyrzykowska, Thermochim. Acta, 179 (1991) 265.
6 K. Takamizawa, Y. Ogawa and T. Oyama, Polymer J., 14 (1982) 441.
7 F. O. Cedeno, M. M. Prieto, A. Espina and J. R. Garcia, J. Therm. Anal. Cal., 73 (2003) 775.
8 F. O. Cedeno, M. M. Prieto, A. Espina and J. R. Garcia, Thermochim. Acta, 369 (2001) 39.
9 S. Wang, K. Tozaki, H. Hayashi, S. Hosaka and H. Inaba, Thermochim. Acta, 408 (2003) 31.
10 H. Inaba, K. Tozaki, H. Hayashi, C. Quan, N. Nemoto and T. Kimura, Physica B, 324 (2002) 63.
11 K. Tozaki, H. Inaba, H. Hayashi, C. Quan, N. Nemoto and T. Kimura, Thermochim. Acta, 397 (2003) 155.
12 S. Hosaka, K. Tozaki, H. Hayashi and H. Inaba, Physica B, 337 (2003) 138.
13 D. A. Ditmars, S. Ishihara, S. S. Chang, G. Bernstein and E. D. West, J. Res. Nat. Bur. Stand., 87 (1982) 159.
14 E. B. Sirota, H. E. King Jr., D. M. Singer and H. H. Shao, J. Chem. Phys., 98 (1993) 5809.
15 E. B. Sirota and D. M. Singer, J. Chem. Phys, 101 (1994) 10873.
16 B. M. Ocko, X. Z. Wu, E. B. Sirota, S. K. Sinha, O. Gang and M. Deutsch, Phys. Rev. E, 55 (1997) 3164.
17 X. Z. Wu, E. B. Sirota, S. K. Sinha, B. M. Ocko and M. Deutsch, Phys. Rev. Lett., 70 (1993) 958.
18 H. Z. Li and T. Yamamoto, J. Chem. Phys., 114 (2001) 5774.
19 T. Shimizu and T. Yamamoto, J. Chem. Phys., 113 (2000) 3351.
20 M. Kawamata and T. Yamamoto, J. Phys. Soc. Japan, 66 (1997) 2350.
21 G. B. Bommarito, W. J. Foster and P. S. Pershan, J. Chem. Phys., 105 (1996) 5265.